



## ORIGINAL ARTICLE

# Comparative study of steel-concrete composite beams for railway bridges

## *Estudo comparativo de soluções para vigas mistas empregadas em obras de arte especiais ferroviárias*

Ruan Richelly Santos<sup>a</sup> Hermes Carvalho<sup>b</sup> Rodrigo Felipe Santos<sup>c</sup> Túlio Nogueira Bittencourt<sup>a</sup> Rodrigo Barreto Caldas<sup>b</sup> <sup>a</sup>Universidade de São Paulo – USP, Escola Politécnica, Departamento de Engenharia de Estruturas e Geotécnica, São Paulo, SP, Brasil<sup>b</sup>Universidade Federal de Minas Gerais – UFMG, Departamento de Engenharia de Estruturas, Belo Horizonte, MG, Brasil<sup>c</sup>Universidade Federal de Viçosa – UFV, Departamento de Engenharia Civil, Viçosa, MG, Brasil

Received 14 September 2022

Revised 20 March 2023

Accepted 23 May 2023

Corrected 27 March 2024

**Abstract:** Steel-concrete composite bridges are a popular solution due to the structural benefits of both steel and concrete. The typical system of a concrete slab and steel I-girders for small and medium-span bridges often displays the most economical results. However, other solutions emerge as innovative alternatives for bridge construction, such as composite beams with composite dowels and pre-cambered composite beams. This paper aims to develop a comparative study of these composite beam solutions to delimitate their efficiency, performance, and economy. Thus, a case study for the superstructure of a two-way simply supported railway bridge is detailed to define the composite beam's performance indicators. The innovative alternatives presented benefits when compared to the traditional system, demonstrating the positive impact of their use on bridges.

**Keywords:** steel-concrete composite beams, railway bridge, composite dowels, pre-cambered composite beams.

**Resumo:** Obras de arte especiais com elementos estruturais mistos de aço e concreto consistem em uma solução popular, uma vez que tais elementos combinam os benefícios estruturais do aço e do concreto. Em pontes de pequenos e médios vãos, a solução que usualmente garante resultados econômicos interessantes é composta por uma laje de concreto sobre vigamento de aço em perfis I. Outras opções que despontam como alternativas eficientes na construção de obras de arte especiais são o sistema de vigas com conectores de cisalhamento em chapa de aço contínua recortada e o sistema de vigas mistas preflexionadas. Diante disso, o presente trabalho tem por objetivo a realização de um estudo comparativo das diferentes soluções de vigas mistas a fim de delimitar a performance das soluções propostas. Para tanto, o estudo de caso da superestrutura de uma ponte ferroviária de duas vias com vão biapoiado é apresentada em detalhes para definir os indicadores de desempenho das soluções. As soluções de vigas mistas propostas apresentaram vantagens quando comparadas com o sistema tradicional, demonstrando o impacto positivo de seu uso no contexto das obras de arte especiais.

**Palavras-chave:** vigas mistas de aço e concreto, pontes ferroviárias, conectores em chapa de aço contínua recortada, vigas mistas preflexionadas.

**How to cite:** R. S. Santos, H. Carvalho, R. F. Santos, R. B. Caldas, and T. N. Bittencourt, "Comparative study of steel-concrete composite beams for railway bridges," *Rev. IBRACON Estrut. Mater.*, vol. 17, no. 3, e17302, 2024, <https://doi.org/10.1590/S1983-41952024000300002>

**Corresponding author:** Ruan Richelly Santos. E-mail: [ruanrichelly@usp.br](mailto:ruanrichelly@usp.br)

**Financial support:** CNPq (grant # 132581/2018-3), FAPEMIG (grant # APQ-01770-18 and APQ-02988-21), FAPESP (grant # 2020/02350-2).

**Conflict of interest:** Nothing to declare.

**Data Availability:** The data that support the findings of this study are available from the corresponding author, RRS, upon reasonable request.

This document has an erratum: <https://doi.org/10.1590/S1983-41952024000300011>



This is an Open Access article distributed under the terms of the Creative Commons Attribution License, which permits unrestricted use, distribution, and reproduction in any medium, provided the original work is properly cited.

## 1 INTRODUCTION

Bridges are a critical part of transport infrastructure, forming essential links on highways and railways to overcome obstacles, such as valleys, rivers, and roads. Thus, they contribute significantly to the economy and social welfare, consisting of structures with complex design and constructive processes. Due to the growing demand for more economical, efficient, and sustainable bridges, studying constructive methods that provide such attributes has become necessary. In this sense, steel-concrete composite bridges have been widely used worldwide for their remarkable structural performance, combining the benefits of steel and concrete elements. The shear connection in these structures allows the optimized use of both materials, improving stiffness and strength.

For small and medium-span bridges with shear connectors, the typical solution of a concrete slab and steel I-girders (Figure 1a) often displays the most economical results. Nevertheless, other solutions, such as steel-concrete composite beams with composite dowels (Figure 1b) and pre-cambered composite beams (Preflex beams, Figure 1c), emerge as innovative alternatives for bridge construction. The filler-beam deck system is also a commonly employed solution for small to medium-span railway bridges. The method main advantage resides in its low constructive depth associated with a high load capacity, aesthetics, stiffness, and easy execution and maintenance. Additionally, the system configuration eliminates the need for shear connectors if certain geometric conditions are met and the mill scale on the steel surface is removed [1]. However, despite its benefits, their verification is not within the scope of this paper, which focuses on comparing the composite beams cross-section displayed in Figure 1, especially to allow the comparison regarding shear connection use.

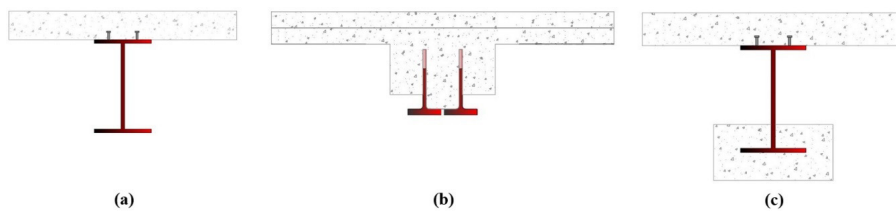


**Figure 1.** Composite beams cross-section examples: (a) traditional solution, (b) beam with composite dowels, (c) pre-cambered composite beam.

The continuous shear connectors, also known as composite dowels, are a new form of shear connectors for composite beams, replacing headed studs for the transference of shear forces between the steel section and concrete slab. This type of connector is usually made of steel plates welded on the upper flange of steel beams or fabricated directly out of the web of steel beams by gas cutting [2]. This paper will focus on the composite dowels manufactured from the web of a steel beam (Figure 2). The solution provides a way to overcome the inherent complexities of installing stud bolts and enables an economical construction form of the composite beam without the upper steel flange. These characteristics result in an economical, rationalized, and time-saving constructive process [3].

Compared to headed studs, the main advantage of composite dowels is the higher load-bearing capacity for static and cyclic load and ductility, a relevant feature for bridge infrastructure [3], [4]. Furthermore, the gas cutting procedure adopted to obtain the continuous shear connectors can provide a system without welds, which increases the beam fatigue capacity. Due to the high degree of industrialization, simple production, quickly enabling placement of reinforcing bars and fast installation on site, the composite beam system with composite dowels is increasingly used in European bridges. Thus, the solution consists of a consolidated constructive method for bridges and an innovative alternative for small and medium spans [3], [5].

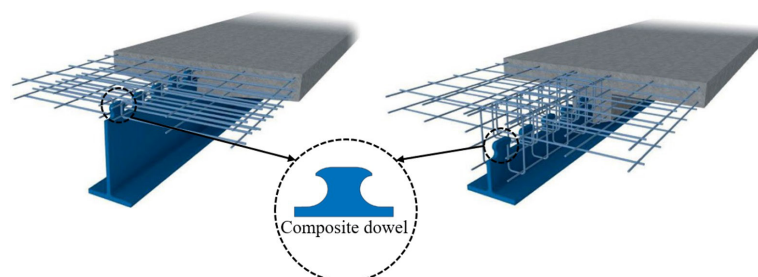


**Figure 2.** Steel-concrete composite beams with composite dowels (Adapted from Feldmann et al. [4]).

On the other hand, the pre-cambered composite beam system, commonly known as the Preflex beam, consists of a kind of prestressed composite beam. This system is composed of a steel I-girder with a bottom flange encased by reinforced concrete, which is fabricated by the following process: the steel I-girder is bent under preflexion loading and, during this step, high-strength concrete is cast in its tensile flange. After the concrete hardening, the loads are removed, and then compressive prestresses are induced in the bottom flange concrete as the beam regains part of its original shape (Figure 3). The structure can then be transported to the site, where the top and web concrete are poured in situ to complete the pre-cambered beam [6], [7].

The Preflex beam constructive configuration ensures stiffness, flexural strength, and slenderness gains. In addition, the technology provides an alternative for structures that demand slender beams in long spans, exhibiting advantages when deflections and vertical clearance must be limited. The system also offers excellent fire resistance and high fatigue performance, which justifies its use in bridge construction [8], [9]. The technology has been employed in large buildings and road and rail bridges. It is particularly interesting to build rail bridge decks of small spans but with a high slenderness ratio when the limitation of deflections under service load can be the most critical condition to satisfy the design [7]. Thus, the pre-cambered composite beams become economically attractive when strict limitations on clearance dictate the use of a slender structure.



Figure 3. Pre-cambered composite beams, Preflex [10].

In this context, steel-concrete composite beams with composite dowels and pre-cambered beams benefit bridge construction, enabling more economical and efficient solutions than traditional systems composed of a concrete slab and steel I-girders. Thus, the comparative study of these constructive alternatives, focusing on delimiting their performance indicators and defining a script for design and construction, becomes relevant and contributes to their dissemination. The current standards do not fully contemplate the design procedure for the composite beams with continuous shear connectors and the pre-cambered composite beams. Furthermore, there is a lack of studies comparing the different solutions and displaying the best alternative for different cases.

Given the benefits of these alternative constructive configurations, this paper aims to develop a comparative study of the different solutions for composite beams with shear connectors to delimitate their efficiency and economy. Developing guidelines for designing and executing these systems [11], [12] contribute to their dissemination in countries such as Brazil, where their application is non-existent. Thus, case studies have been carried out according to the Eurocode design provisions [13]. Nevertheless, to fill the design gaps present in the current standards, the Z-26.4-56 [14] technical approval has covered the composite dowels design. Also, Morano and Mannini's method [7] has covered the procedures for calculating stresses and deflections due to creep and shrinkage effects for Preflex beams.

## 2 DESIGN OF STEEL-CONCRETE COMPOSITE BEAMS

This section focuses on displaying the design of the three steel-concrete composite beam solutions objects of study of this paper (Figure 1): conventional solution of a concrete slab and steel I-girders, composite beam with composite dowels, and pre-cambered composite beams. The Eurocode standards are recognized internationally, providing information for the design and construction of bridges. The EN 1994-2:2005 [13] presents the principles and requirements for the safety, serviceability, and durability of composite steel and concrete structures, together with

specific provisions for bridges. Thus, the instructions proposed by the Eurocode were employed during the study and design of the traditional solutions. Nonetheless, they do not fully cover all the information for the design of the beams with composite dowels and Preflex beams. The additional provisions necessary for the design were obtained by technical approvals and analytical models in the literature, such as the Z-26.4-56 [14] technical approval for the continuous shear connectors and Morano and Mannini's method [7] for the Preflex beam.

## 2.1 Traditional solution: concrete slab and steel I-girders

This solution consists of a steel I-girders set, usually equally spaced from each other, that supports a reinforced concrete slab (Figure 4), being common for road and rail bridges. The typical deck slenderness ratio ( $L/H$ , where  $L$  is the main span length and  $H$  is the deck height) varies between 20 and 30, while the transverse spacing between the beams is usually around 2.50 to 4.00 meters [15], [16].

The steel girders can be made of laminated or welded profiles. Usually, laminated profiles are economically viable for spans of up to 30 meters, while welded profiles are recommended between 20 and 40 meters, although there are cases where spans exceed 90 meters. The most significant advantage of welded profiles is the possibility of asymmetrical sections and hybrid beams made with steels of different steel strengths for the web and flange [17]. The manufacturing process usually restricts the dimensions of laminated profiles. For example, in Brazil, laminated sections are limited to 600 mm in height, which contributes to restraining the use of these profiles on bridges with short spans. Thus, this paper will consider only welded profiles for the conventional solution design.

The span dimension directly impacts the selection of bridge type to be built. For small spans up to 20 meters, concrete bridges are usually more economical than composite bridges since the self-weight is still not a limiting factor for execution and structural behavior. However, for small and medium spans from 25 to 50 meters, the steel-concrete composite beam with steel I-girders becomes economically competitive with reinforced concrete bridges. As the span increases, concrete construction becomes heavy, while composite structures with more slender parts become particularly interesting [5].

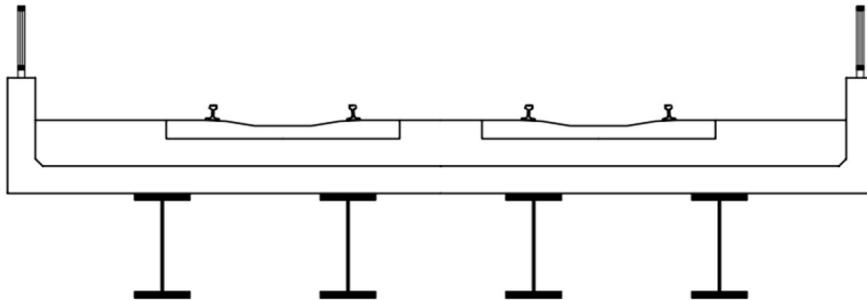


Figure 4. Typical section of a composite bridge with steel I-girders [18].

The design of the traditional solution is carried out following the EN 1994-2:2005 [13], which is based on the limit state concept used in conjunction with a partial factor method. Other standards, however, complement the EN 1994-2:2005 [13], in particular: EN 1994-1-1:2004 [19] and EN 1990:2002 [20]; EN 1993-1-1:2005 [21], EN 1993-1-5:2006 [22], EN 1993-1-9:2005 [23] and EN 1993-2:2006 [24], for the design of steel elements; EN 1992-1-1:2004 [25] and EN 1992-2:2005 [26], for the design of concrete elements.

For Ultimate Limit States (ULS), the following verifications are applied: i) resistance of the beam cross-section to bending, vertical shear, and the interaction between these forces; ii) resistance to lateral-torsional buckling; iii) resistance to shear buckling and in-plane forces applied to webs; iv) resistance to longitudinal shear, focusing on the headed studs connectors; v) resistance to fatigue.

The following checks are stipulated for Service Limit States (SLS): i) stress limitations for structural steel, reinforcing steel, and concrete; ii) control of the web breathing effect on the profile web. This effect causes cyclic deformations that can induce fatigue cracks in the element; iii) concrete cracking control; iv) displacements (displacement limit based on comfort level and acceleration limit); v) resistance to longitudinal shear for service loads.

The demonstration of the design formulations presented in Eurocode provisions is out of the scope of this paper. More information regarding design and construction can be found on the aforementioned standards. This paper will address the additional formulations necessary to design the composite dowels and calculate the stresses and deflections for Preflex beams.

## 2.2 Composite beam with composite dowels

The first steel-plated shear connector dates from 1987, known as Perfobond [27]. These devices were shaped with circular holes and welded on a steel profile’s superior flange. Other solutions with drilled holes were developed with the inclusion of cuts to promote an additional anchor effect. Connector solutions were proposed by making an open cutout in a single cutting line. These connectors with regular open-shaped geometry are known as composite dowels and may present different shapes. For these connectors, the shear loads are mainly transferred by interactions of steel and concrete dowels, improving the shear connection ductility [28].

Advancing the composite dowels research, Seidl et al. [29] proposed an optimized solution to introduce a higher industrialization level and reduce the time for installation in the field. Thus, allowing the development of new connectors for composite bridges, clothoidal and puzzle. The study guided the development of the Z-26.4-56 [14] guidelines, which stipulate the design and constructive specification for the composite dowels puzzle and clothoidal. Figure 5 displays the development timeline for the steel-plated connectors.

The use of beams with composite dowels results in a particularly interesting system for highway and railway bridges due to their high fatigue resistance. Furthermore, the system increases construction efficiency due to its manufacturing process and can reduce the amount of steel and welding employed in the design. Due to its economic advances, the solution is being used for bridge construction, especially in Europe [30]. It is possible to notice that, in general, composite beams with composite dowels are usually adopted for bridges with small and medium spans, between 12 and 30 meters, with a deck slenderness ratio ranging from 15 to 25 [11].

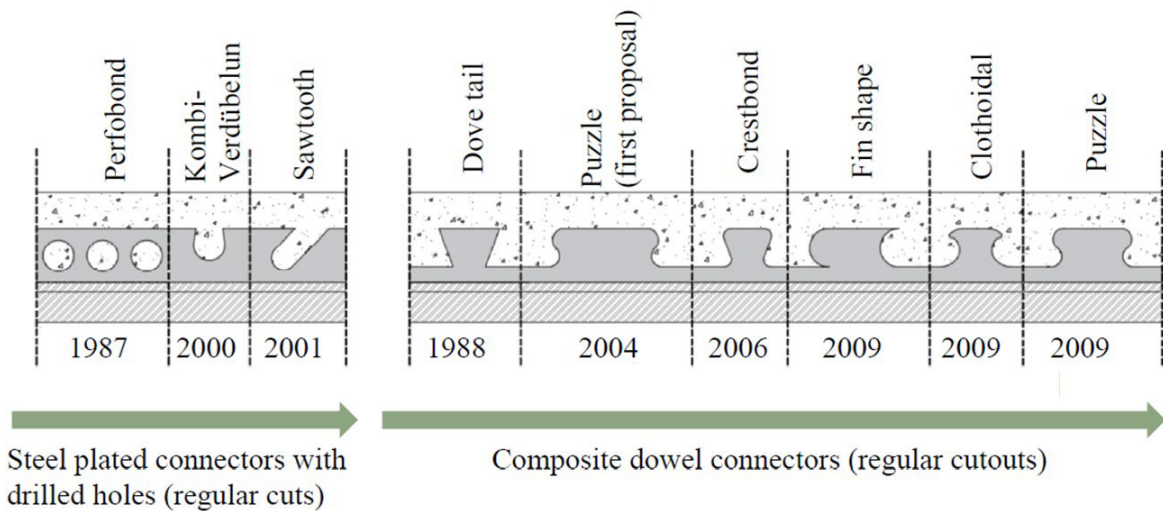


**Figure 5.** Development timeline of steel-plated connectors with drilled holes and composite dowel connectors (Adapted from Cardoso et al. [28]).

### 2.2.1 Z-26.4-56 technical guidelines

Regarding composite dowels, the Z-26.4-56 [14] is the most developed technical regulation. This guideline is compatible with the Eurocode standards, covering only the items not prescribed in these codes. The Z-26.4-56 [14] defines the calculation procedure for Puzzle (PZ) and Clothoidal (CL) connectors (Figure 6). The connectors geometry is a function of the spacing between the openings ( $e_x$ ), which varies from 150 to 500 mm.

In the design formulae, the steel plate web thickness ( $t_w$ ) must be limited between 6 and 40 mm, with a  $t_w/h_D$  ratio between 0.08 and 0.50. The minimum perpendicular distance between two steel plates ( $e_y$ ) must be 120 mm to ensure sufficient space for laying the reinforcement. In addition, the concrete top cover ( $c_o$ ) and bottom cover ( $c_u$ ) must be at least 20 mm thick. Regarding the materials used, steel profiles of classes S235, S355, and S460 are allowed ( $f_y = 235, 355, \text{ and } 460$  MPa, respectively) and concrete with characteristic strength ( $f_{ck}$ ) from 20 and 60 MPa. Figure 7 and Figure 8 display the geometry notation adopted in this paper.



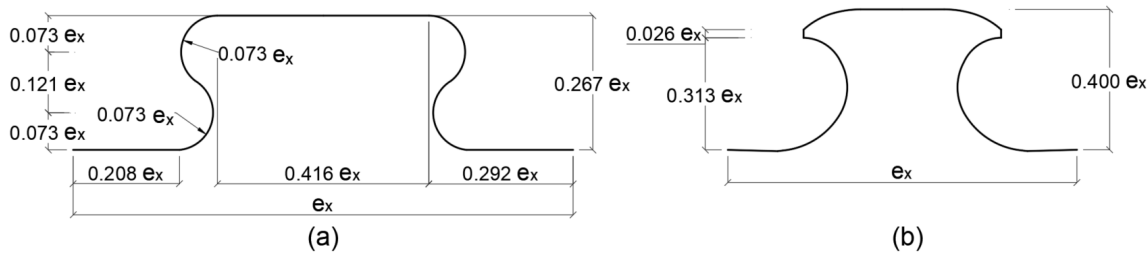


Figure 6. Composite dowels geometry: (a) puzzle, (b) clothoidal.

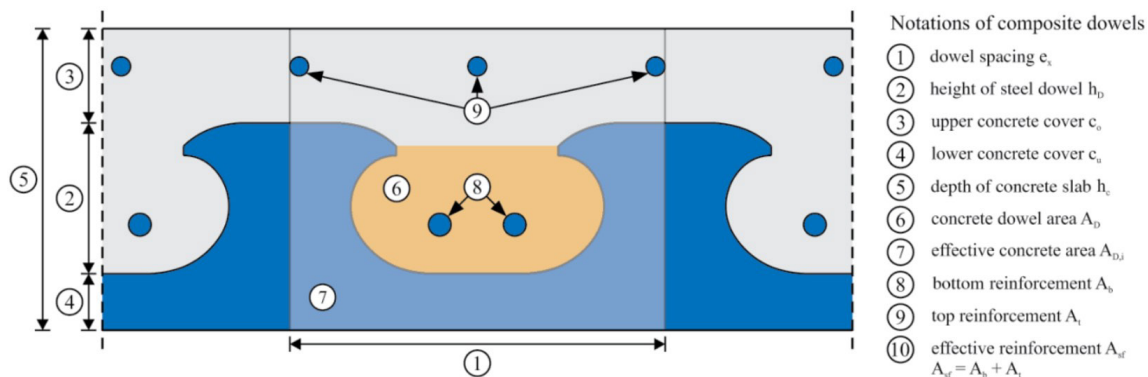


Figure 7. Notation for the section along a composite dowel [4].

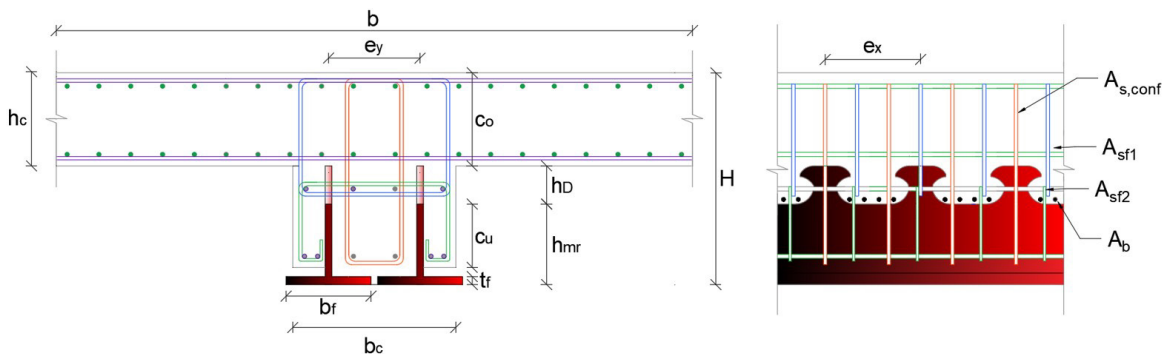


Figure 8. Geometry notation for the double composite beam with composite dowels.

### 2.2.1.1 Longitudinal shear resistance

The composite dowels are subjected to three failure modes: concrete shearing, concrete pry-out, and steel failure (Figure 9). Equation 1 gives the strength capacity for PZ and CL connectors. Thus, the longitudinal shear resistance ( $P_{Rk}$ ) is the smallest value between concrete shearing ( $P_{sh,k}$ ), concrete pry-out ( $P_{po,k}$ ) and steel failure ( $P_{pl,k}$ ).

$$P_{Rk(CL,PZ)} = \min \begin{cases} P_{sh,k} = \eta_D e_x^2 \sqrt{f_{ck}} (1 + \rho_D) \\ P_{po,k} = \chi_x \chi_y 90 h_{po}^{1.5} \sqrt{f_c} (1 + \rho_{D,i}) \\ P_{pl,k} = 0.25 e_x t_w f_y \end{cases} \quad (1)$$

The geometry-dependent reduction factor  $\eta_D$  ( $\eta_{D,CL} = 3 - e_x/180$ ,  $\eta_{D,PZ} = 2 - e_x/400$ ) considers the two merged shear planes in cases of large openings. The opening reinforcement ratio ( $\rho_D$ ) is given by the ratio between  $E_s A_b$  and  $E_{cm} A_D$ , in which  $E_s$  and  $E_{cm}$  are the steel and concrete elastic modulus, respectively. The term  $f_y$  is the steel yield strength.

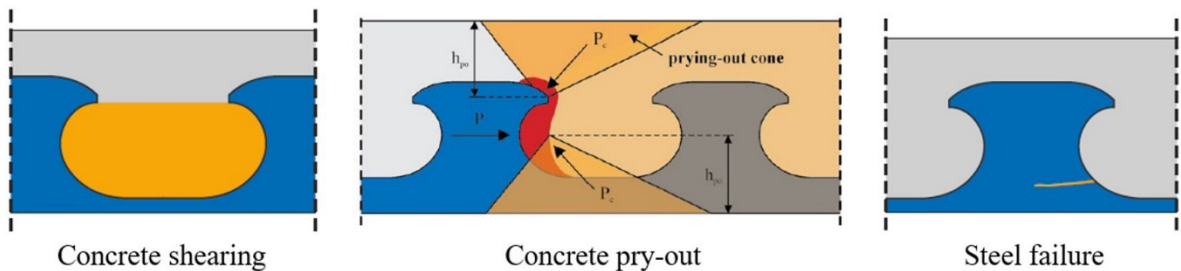


Figure 9. Composite dowels failure modes [2], [4].

The concrete cone height ( $h_{po}$ ) is given by the smallest value between  $(c_o + 0,07e_x)$  and  $(c_u + 0,13e_x)$ . The effective reinforcement ratio ( $\rho_{D,i}$ ) is given by the ratio between  $E_s A_{sf}$  and  $E_{cm} A_{D,i}$ , where  $A_{sf}$  is the effective reinforcement area defined as the sum of the lower reinforcement area ( $A_b$ ) and the upper reinforcement area ( $A_t$ ). The reduction factors  $\chi_x$  and  $\chi_y$  consider the concrete cones overlapping effect in the longitudinal and transverse directions, respectively.  $\chi_x$  is applied when the connector has a longitudinal spacing ( $e_x$ ) less than  $4,5h_{po}$ , Equation 2.  $\chi_y$  is adopted when the composite dowels are arranged in parallel with  $e_y$  spacing less than  $9h_{po}$ , Equation 3.

$$\chi_x = e_x / 4.5h_{po} \leq 1 \tag{2}$$

$$\chi_y = (e_y / 9h_{po} + 1) / 2 \leq 1 \tag{3}$$

The concrete horizontal splitting failure mode may occur for beam sections in which the composite dowels constitute part of a T-shaped external reinforcement section. A minimum area for confinement stirrups should be defined to avoid this failure, as displayed by Equation 4. In order to guarantee that the confinement stirrups enclose the concrete compression strut, these elements must follow the constructive requirements of Figure 10.

$$A_{s,conf} = 0.3P / f_{sd} \tag{4}$$

where  $f_{sd}$  is the design yield strength of the confinement stirrups.

The transverse reinforcement required ( $A_b$ ) must be determined according to a 45° strut-and-tie model, as described by Equation 5.

$$A_b = 0.5P / f_{sd} \tag{5}$$

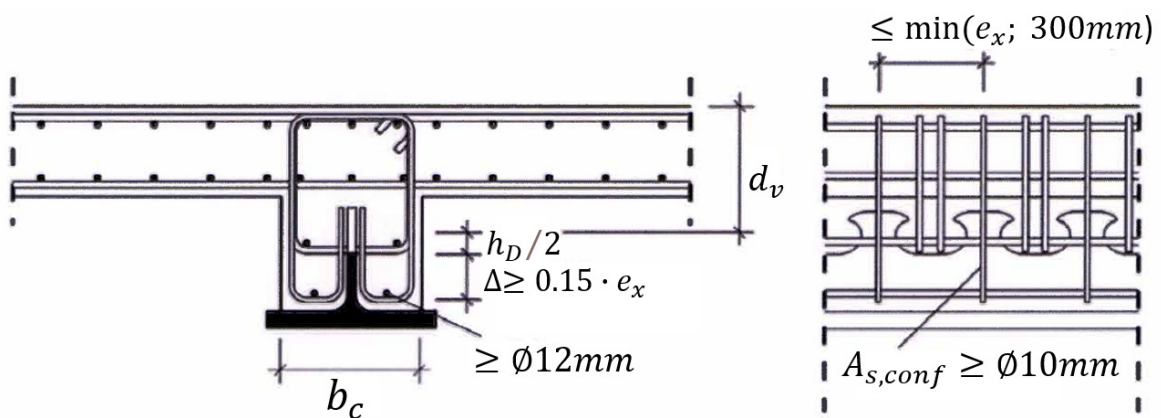


Figure 10. Reinforcement details in composite girder with reinforced concrete web and composite dowels [14].

### 2.2.1.2 Fatigue strength

In the steel fatigue verification process, the stress amplitude equivalent to 2 million cycles at the hotspot is determined taking account of the fatigue load model and compared with material fatigue strength, which can be described by the fatigue strength curve of detail category 125 or 140, following the EN 1993-1-9:2010 [23]. The nominal stresses are defined as longitudinal shear stresses (local effects) and normal stresses (global effects) at the dowel base, as represented in Equation 6.

$$Ds = \left| k_{f,L} \frac{DVs_y}{I_y t_w} \right| + \left| k_{f,G} \left( \frac{DN}{A} + \frac{DM}{I_y} z_D \right) \right| \leq 1.3f_y \quad (6)$$

The local ( $k_{f,L,CL} = 7.3$ ;  $k_{f,L,PZ} = 8.6$ ) and global ( $k_{f,G,CL} = 1.5$ ;  $k_{f,G,PZ} = 1.9$ ) stress concentration factors were determined in the Z-26.4-56 [14]. The terms  $S_y$  and  $I_y$  are the composite section's first and second moment of area, respectively.  $z_D$  is the distance between the composite section's neutral axis to the centroid of the effective concrete area.

In order to secure a rigid shear connection and prevent the cyclic concrete pry-out in service, the section resistance to longitudinal shear is given according to Equation 7.

$$P_{LD,ser} = \min \left\{ \begin{array}{l} 0.7P_{Rk} \\ P_{cyc} = 3.1t_w h_D f_{ck} \end{array} \right. \quad (7)$$

## 2.3 Pre-cambered composite beams

The pre-cambered composite beams, also known as Preflex beams, were invented in the 50s. The main structural innovation of this system is due to the presence of a prestressed high-strength concrete flange in the steel profile lower flange. It is essential to notice that during the manufacturing process, the elements of the Preflex beams are subjected to greater forces than those they will be exposed to during their life cycle. Thus, extensive constructive quality control is necessary to guarantee the system's safety and efficiency [8].

The pre-cambered composite beams have been widely adopted in buildings and bridge construction. Due to its characteristics, this solution is especially efficient for developing railway infrastructure. The technology provides an alternative for structures that demand slender beams in long spans, exhibiting advantages when deflections and vertical clearance must be limited. The system also offers excellent fire resistance and high fatigue performance, which justifies its use in bridge construction, achieving spans greater than 45 meters long [31].

The Preflex beams analysis follows the concepts proposed by standards. However, additional verifications present in the literature are necessary due to the different stages of its construction process. Among them, we can mention a stress verification for each step and the method for calculating creep and shrinkage effects specific to Preflex beams presented by Morano and Mannini [7].

### 2.3.1. Stress calculations

Stresses in the structure are verified for different stages of the constructive process: i) preflexion loads application; ii) release of the applied loads and concrete casting in the tensile flange; iii) addition of the concrete slab self-weight; iv) service stage, including live load acting in the structure.

For each stage, the stresses on the Preflex beam's elements are compared with the materials' allowable stresses. This evaluation is made for the constructive process and service conditions. Different authors, such as Portela et al. [8] and Mannini [32], proposed stress limits for this technique. This paper focused on adopting the definitions proposed by Portela et al. [8] to verify the stresses on structural steel, concrete, and reinforcing steel stresses.

### 2.3.2. Concrete creep and shrinkage verification

The complex Preflex beam configuration, composed of a steel profile encased by concrete elements cast at different times and usually with different mechanical properties, results in laborious calculations to determine the behavior caused by the concrete long-term creep and shrinkage effects. In order to simplify these calculations while maintaining an adequate level of accuracy for practical applications, Morano and Mannini [7] developed an analysis method for composite beams using concrete age-adjusted modular ratios that allow the estimation of time-dependent stresses in the



concrete flange due to creep and shrinkage. The procedure consists of solving four algebraic equations in which the unknown variables are the forces acting on steel and concrete, as described in Equations 8-11. The internal and external forces are considered positive according to the convention presented in Figure 11.

$$N_s(t) + N_c(t) = 0 \tag{8}$$

$$M_s(t) + M_c(t) + N_c(t) \cdot d = M \tag{9}$$

$$\frac{N_s(t)}{E_s A_s} + \frac{M_s(t)}{E_s I_s} d = \frac{\eta_N(t) N_c(t)}{A_c E_s} \tag{10}$$

$$\frac{M_s(t)}{E_s I_s} = \frac{\eta_M(t) M_c(t)}{E_s I_c} \tag{11}$$

$N_s, N_c$  are the axial force on the steel and concrete section, respectively.  $M_s, M_c$  are the bending moments on the steel and concrete.  $I_s$  is the steel section second moment of area.  $M$  is the external bending moment, while  $d$  is the distance between the neutral axis of the steel and concrete elements. Finally,  $P$  is the prestress force applied in the cross-section.

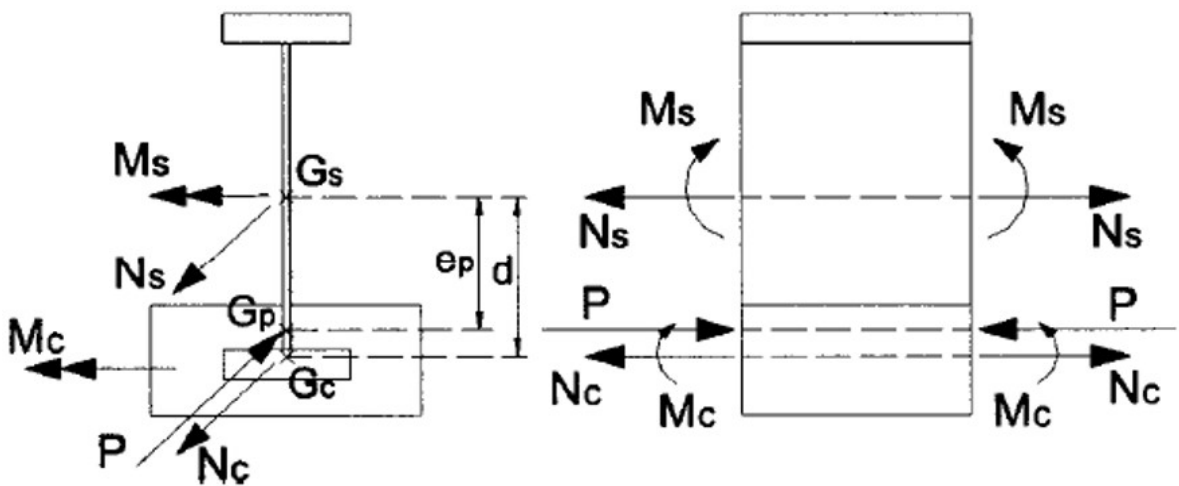


Figure 11. Sign convention for the cross-section's internal and external effects [7].

From manipulations of the equilibrium and compatibility equations, the modular ratio for axial force,  $\eta_N(t)$ , and the modular ratio for bending moment,  $\eta_M(t)$ , can be specified by Equations 12 and 13.

$$\eta_N(t) = \frac{\zeta(t_0, t) \cdot \left( \frac{A_c}{A_s} + \frac{A_c d^2}{I_s} \right) + [(1-\alpha) \cdot \zeta(t_0, t) + \alpha] \cdot n_i}{n_i + \frac{A_c}{A_s} + \frac{A_c d^2}{I_s} - n_{28} \alpha [\zeta(t_0, t) - 1]} n_{28} \tag{12}$$

$n_i$  is the modular ratio for the aged concrete at the date of application of the loading,  $n_i = E_s/E_c(t_0)$ .  $n_{28}$  is the modular ratio for concrete aged 28 days,  $n_{28} = E_s/E_{28}$ .  $\alpha$  is the calibrated parameter for axial force.  $\zeta(t_0, t)$  is the term that defines the deformation for a time  $t$  caused by a unit of constant stress acting from time  $t_0$  to  $t$ . This term can be expressed as a function of the creep coefficient,  $\varphi(t_0, t)$ . The creep coefficient is usually defined by technical standards.

$$\eta_M(t) = \frac{\zeta(t_0, t) - \alpha_M [\zeta(t_0, t) - 1] \cdot \gamma}{1 - n_{28} \alpha_M [\zeta(t_0, t) - 1] \cdot \beta(t)} n_{28} \tag{13}$$

$\alpha_M$  is the calibrated parameter for bending stress.  $\beta(t)$  is a function dependent on the coefficient for axial force  $\eta_N(t)$ , expressed by Equation 14.

$$\beta(t) = \frac{n_i + \frac{A_c}{A_s}}{n_N(t) + \frac{A_c}{A_s}} \cdot \frac{n_N(t) + \frac{A_c}{A_s} + \frac{A_c d^2}{I_s}}{\frac{I_c}{I_s} \left( n_i + \frac{A_c}{A_s} \right) + n_i \left( n_i + \frac{A_c}{A_s} + \frac{A_c d^2}{I_s} \right)} \quad (14)$$

$\gamma$  a term originated from the equations manipulation, defined as Equation 15.

$$\gamma = \frac{n_i \left( n_i + \frac{A_c}{A_s} + \frac{A_c d^2}{I_s} \right)}{\frac{I_c}{I_s} \left( n_i + \frac{A_c}{A_s} \right) + n_i \left( n_i + \frac{A_c}{A_s} + \frac{A_c d^2}{I_s} \right)} \quad (15)$$

Regarding the concrete shrinkage, the pre-cambered composite beam deformations are restricted by the stiffness of the connection with the steel profile. Thus, the modular ratios for the shrinkage effects for axial force and bending moment are defined by Equations 16 and 17, respectively.

$$\eta_N(t) = n_{28} [(1 - \alpha) \cdot \zeta(t_i, t) + \alpha] \quad (16)$$

$$\eta_M(t) = n_{28} [(1 - \alpha_M) \cdot \zeta(t_i, t) + \alpha_M] \quad (17)$$

### 3 CASE STUDY: STEEL-CONCRETE RAILWAY BRIDGE

A case study of a two-way simply-supported railway bridge was developed to evaluate the contributions and performance of the composite beam configurations presented in this paper. Thus, the typical solution of a concrete slab and steel I-girders was compared with the composite beams with composite dowels and pre-cambered composite beams. The deck cross-section for the case study is displayed in Figure 12, which was considered constant along the span.

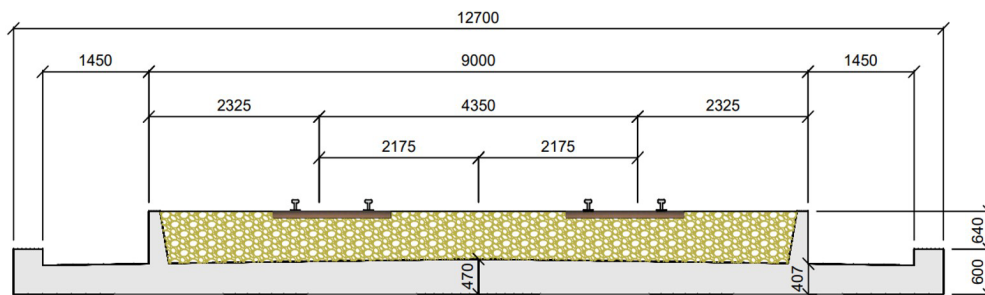


Figure 12. Reference deck cross-section.

In order to keep the case study on the range of small and medium spans, in which the conventional solution and the beams with composite dowels often display the most economical results, spans of 20, 25, and 30 meters were analyzed. For each span length, three different values for the deck slenderness ratio ( $L/H$ ) were defined: 15, 20, and 25. Adopting fixed deck slenderness ratios standardizes the design of the different solutions, enabling the comparison of equal deck heights. Thus, it was possible to specify performance indicators for each constructive system.

A composite beam nomenclature was employed to represent the solution obtained for each system. The classification considered the type of composite beam solution (TRA: traditional solution of concrete slab and steel I-girders; PCB: composite beam with composite dowels; PFX: pre-cambered composite beam), span length (S20: 20 m; S25: 25 m; S30: 30 m), deck slenderness ratio (LH15, LH20, and LH25 to represent three different slenderness ratios adopted), and steel fabrication method (L: laminated profile; W: welded steel plates). For instance, PFX-S20-LH15-W describes a 20-meter span pre-cambered composite beam with a deck slenderness ratio of 15 and composed of welded steel plates.

### 3.1 Materials and loading characteristics

The dead load was defined from the specific weight of  $25 \text{ kN/m}^3$  for concrete and  $78.5 \text{ kN/m}^3$  for structural steel. For the ballast and waterproofing system,  $18 \text{ kN/m}^3$  was considered applied across the entire deck width with an average height between slab and rails equal to 80 cm. Sound barriers were also provided at the deck extremities, with a self-weight of  $2 \text{ kN/m}^2$  and a height of 4 meters from the concrete slab. For the live load, the LM71 and SW/2 loading models described in EN 1991-2:2003 [33] were employed, considering a train speed of  $160 \text{ km/h}$ . For simplicity, loads were transversally distributed according to Courbon’s method [34], as represented in Figure 13. The composite beam design was carried out in accordance with provisions presented in section 2 of this paper.

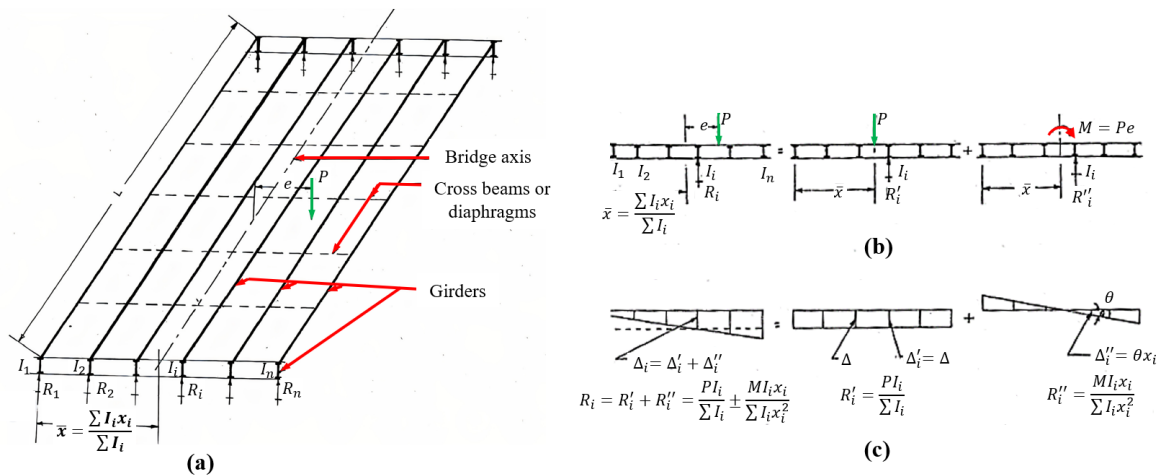


**Figure 13.** Courbon’s method: (a) girder bridge deck eccentrically loaded, (b) transverse section with equivalent loading, (c) transverse deflection profile and girder reaction (Adapted from Binjola [34]).

### 3.2 Design of steel-concrete composite beams

All the suitable formulations and code checks, based on the design proposed by the Eurocode provisions and additional design verifications described in Section 2, were implemented in an electronic spreadsheet linked to commercial steel profile tables. In addition, the steel plate dimensions could be inserted manually, allowing the evaluation of welded cross-sections. The composite beams were designed to obtain the lowest steel weight per deck area. Figure 14 displays a flowchart with the steps adopted to achieve the composite beams for each solution. The employed design formulations can be found in more detail in Santos [11].

For the design, the following approach was adopted: first, the total height of the composite beam was adjusted to adapt to the deck slenderness ratio ( $L/H$ ) values. Then, the profile web thickness was stipulated to meet the verifications for the vertical shear forces on the beam. Finally, the flange dimensions and the number of beams were adjusted to meet all ultimate, service, and fatigue limit state checks.

A solution consisting of a double steel profile section was employed for the composite beam with composite dowels. This solution guarantees constructive and aesthetic advantages. In addition, the steel beams serve as concrete forms, saving materials and labor time. For the concrete elements, concrete with  $f_{ck}$  of 50 MPa was adopted for the deck slab of all solutions. For the pre-cambered composite beams, for the concrete encasing the steel profile bottom flange a  $f_{ck}$  of 90 MPa was considered. The reinforcing steel was adopted with a  $f_y$  of 500 MPa, while for the structural steel a  $f_y$  of 460 MPa was employed.

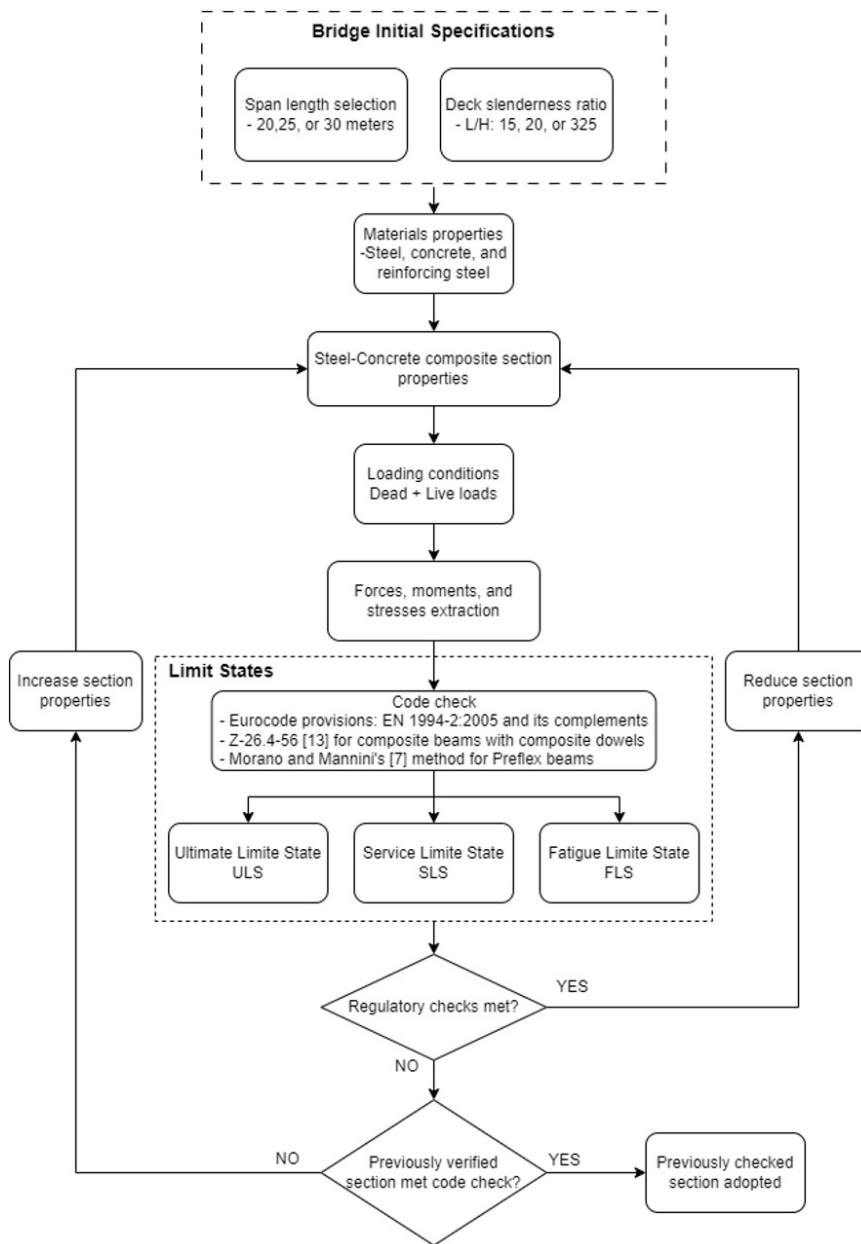


Figure 14. Flowchart for the composite beams design.

### 3.3 Cost analysis

A cost analysis of the different solutions was carried out. The prices of building materials are dynamic, changing over time, location, and even how the products are purchased. Therefore, a simplified analysis was employed, defining each material used for the bridge construction as an equivalent steel amount based on its prices. Table 1 displays the relationship of the materials based on the prices provided by companies from the field in the state of Minas Gerais, Brazil. The cost of materials was stipulated based on a proportion of the price of 1 kg structural steel S460, which received a unitary value. For each material, an equivalent quantity (in kg) of S460 steel was defined based on their prices. Then, the deck costs were compared through the equivalent S460 steel weight per unit of deck area.

Even though it is a simplified cost analysis, it allows comparing the different solutions regarding the cost of the employed materials. The comparison was provided to evaluate the methods by their general performance (without restrictions) and in situations where it is necessary to limit the structure height, either for constructive or aesthetic reasons.

**Table 1.** Equivalent cost for materials.

Material	Equivalent S460 steel
1 kg of structural steel S460, $f_y = 460$ MPa	1.00 kg
1 kg of reinforcing steel, $f_y = 500$ MPa	0.64 kg
1 m <sup>3</sup> of concrete, $f_{ck} = 50$ MPa	50.00 kg
1 m <sup>3</sup> of concrete, $f_{ck} = 90$ MPa	68.00 kg

### 4 RESULTS AND DISCUSSION

The composite beams were designed and optimized according to the definitions proposed in item 3 of this paper. Figure 15 summarizes the geometry notation adopted for the composite beam solutions: traditional solution of a concrete slab and steel I-girders (Figure 15a), composite beam with composite dowels (Figure 15b), and Preflex beam (Figure 15c).

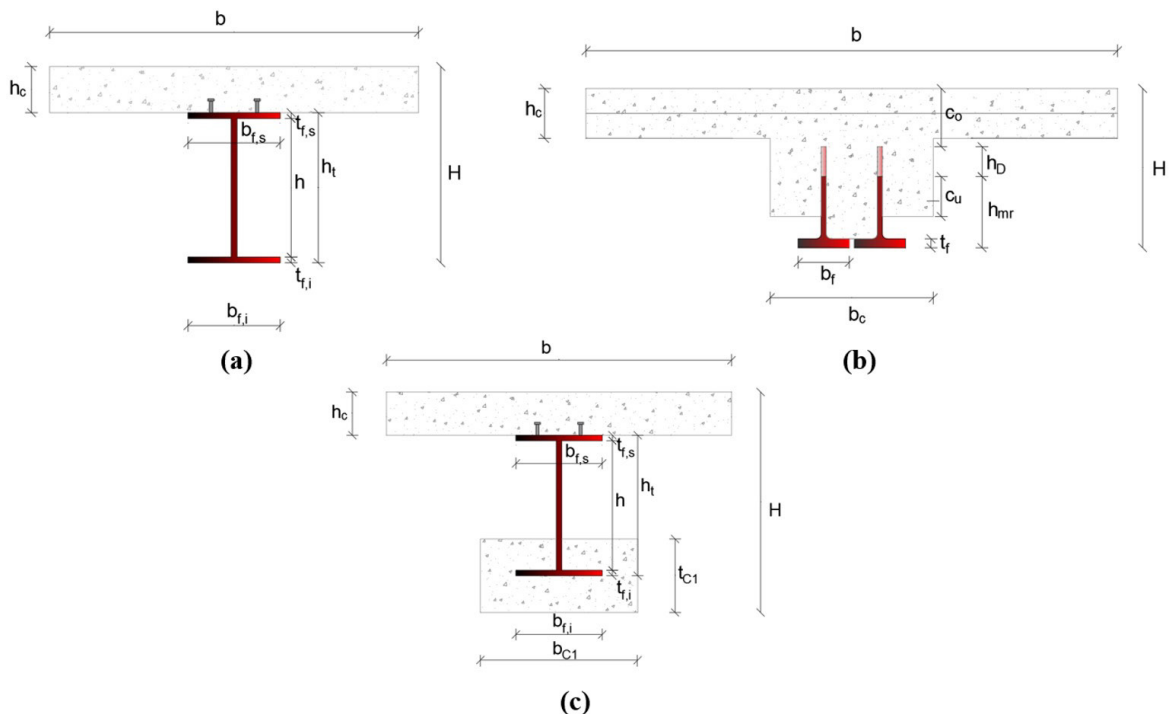


**Figure 15.** Cross-section geometry notation: (a) traditional composite beam; (b) composite beam with composite dowels; (c) pre-cambered composite beam.

#### 4.1 Traditional solution: concrete slab and steel I-girders

Table 2 displays the geometric and constructive information obtained from the case studies, including steel and concrete rates per unit of deck area. The steel rate has a more significant influence on the final cost. Thus, the steel amount is a reasonable parameter for verifying the cost-benefit of the proposed cross-sections. As shown in Figure 16, for the same span, the traditional solution has a lower steel rate for lower values of the deck slenderness ratio ( $L/H$ ).

The peak in steel consumption displayed for an  $L/H$  ratio of 25 indicates that the analyzed solution does not have such a good efficiency when compact sections must be adopted due to height limitations. Thus, a good starting point for the solution pre-design is found at a level close to  $L/H$  of approximately 15. In order to exemplify the case study, Figure 17 illustrates the deck cross-section for the TRA-S20-LH15-W solution, while Figure 18 shows the section's constructive details. In the annex, Appendix A.1 displays the results of essential checks for designing the composite beams for the ultimate, service, and fatigue limit state.

### 4.2 Composite beams with composite dowels

Table 3 presents information regarding the designed composite beams with continuous shear connectors. Appendix A.2 shows the results for the ultimate, service, and fatigue limit states verification. Even though the system is commonly fabricated with laminated profiles, the composite beams were designed as welded plates to provide a better basis for comparison with the other proposed solutions and to fit the technology to Brazil’s technical practice.

For comparison, the laminated section PCB-S20-LH20-L was also analyzed. It is possible to verify in Table 3 that the optimized beam with welded plates (PCB-S20-LH20-W) allowed a considerable reduction in steel consumption for the same application level. Thus, the use of welded plates is an interesting alternative to beams with composite dowels in countries where the manufacturing process of laminated profiles is limited, such as Brazil. However, verifying the connection between steel web and flange for fatigue effects is essential in these cases.

Regarding the structural performance, it was found that the failure mode determining the design was related to the composite dowel fatigue. It was observed during the design the importance of ensuring adequate dimensions for the concrete cover,  $c_o$  and  $c_u$ , which are directly related to the occurrence of pry-out failure. In addition, the impact of the longitudinal spacing between the connectors ( $e_x$ ) was also noted. This dimension is limited by the technical prescription from 150 to 500 mm. Values close to the lower limit favor a pry-out failure, while values that approach the upper limit contribute to the occurrence of a shear failure.

**Table 2.** Geometric information of the sections obtained: traditional solution.

Case	Steel section						Stud bolts			Composite section				
	h (mm)	bf,sup (mm)	tf,sup (mm)	bf,inf (mm)	tf,inf (mm)	tw (mm)	Studs/section	Type	Number of beams	H (mm)	b (mm)	hc (mm)	Steel weight/deck area (kg/m <sup>2</sup> )	Concrete volume/deck area (m <sup>3</sup> /m <sup>2</sup> )
TRA-S20-LH15-W	893.00	450.00	22.40	550.00	44.50	19.00	4	Ø22x150	4	1333.00	3167.50	440.00	124.24	0.44
TRA-S20-LH20-W	560.00	450.00	25.00	580.00	76.00	16.00	4	Ø22x150	6	1000.00	2111.67	440.00	232.44	0.44
TRA-S20-LH25-W	360.00	450.00	22.40	850.00	89.00	37.50	4	Ø22x150	9	800.00	1407.78	400.00	528.78	0.44
TRA-S25-LH15-W	1227.00	450.00	22.40	550.00	52.50	19.00	4	Ø22x150	4	1667.00	3167.50	440.00	150.44	0.44
TRA-S25-LH20-W	810.00	450.00	16.00	600.00	76.00	16.00	4	Ø22x150	7	1250.00	1810.00	440.00	278.16	0.44
TRA-S25-LH25-W	560.00	450.00	22.40	960.00	89.00	19.00	4	Ø22x150	10	1000.00	1267.00	440.00	643.10	0.44
TRA-S30-LH15-W	1560.00	400.00	25.00	550.00	54.00	22.40	4	Ø22x150	4	2000.00	3167.50	440.00	180.18	0.44
TRA-S30-LH20-W	1060.00	450.00	25.00	615.00	82.00	19.00	4	Ø22x150	7	1500.00	1810.00	440.00	345.22	0.44
TRA-S30-LH25-W	760.00	450.00	19.00	1200.00	89.00	16.00	4	Ø22x150	10	1200.00	1267.00	440.00	777.47	0.44

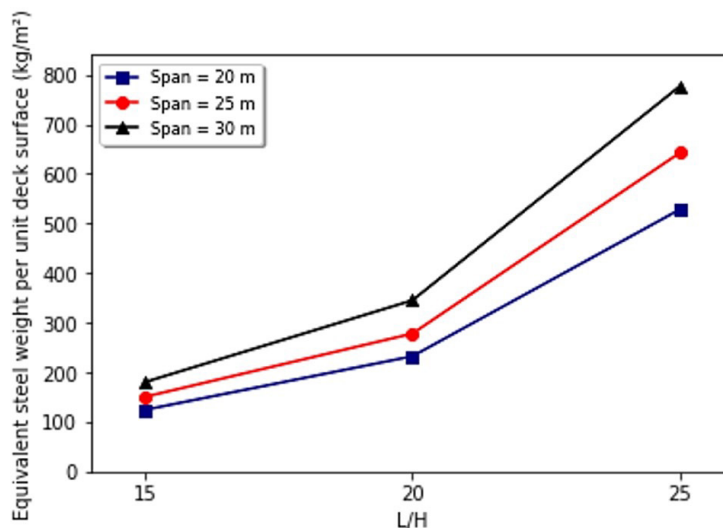


**Figure 16.** Equivalent steel weight per unit deck surface to slenderness ratio.



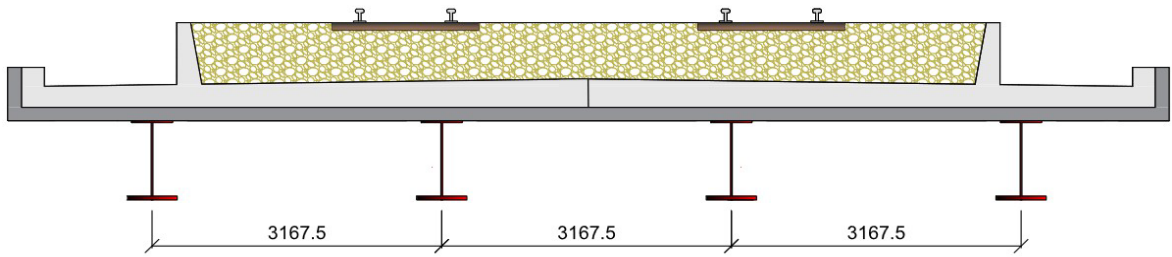


Figure 17. TRA-S20-LH15-W deck cross-section (dimensions in mm).

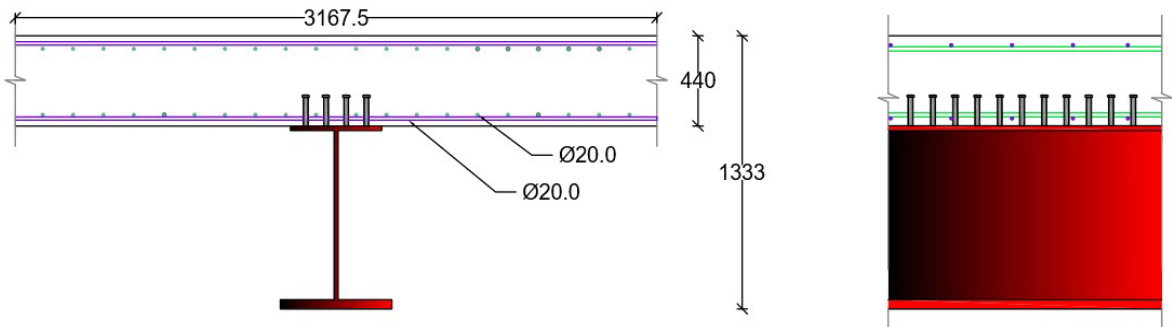


Figure 18. Construction details of TRA-S20-LH15-W solution (dimensions in mm).

From Figure 19, it is possible to observe that between the slenderness ratio of 15 and 20 there is only a slight change in the steel rate. Thus, this characterizes a suitable interval for the solution pre-design. As seen for the system composed of a slab and steel I-girders, there is also an increase in steel consumption for the  $L/H$  ratio of 25. However, compared to the traditional solution, this increment is not so significant, indicating that the beams with composite dowels present a superior performance in this range from an economic point of view. Figure 20 displays the deck cross-section for the PCB-S20-LH20-W solution, while Figure 21 shows the constructive cross-section details.

### 4.3 Pre-cambered composite beams

For this case, different dimensions for the steel plates and bottom flange were evaluated. Table 4 displays the data from the pre-cambered composite beams design. As shown in Table 4 and Figure 22, there is a steel consumption increase when changing the deck slenderness ratio from 15 to 20. This behavior is similar to the one observed in the traditional solution. The steel usage for these first two levels is relatively discrete compared to the steel amount found in the  $L/H$  ratio of 25. In general, it is possible to notice that the reduction in the section's height implies greater steel consumption since it is necessary to use more robust profiles to compensate for the limited size.

For the design checks, it is possible to notice that the vertical shear determines the design for 20 and 25 meters spans (Appendix A.3). As for the 30 meters span, the design is conditioned by the displacements at midspan. Figure 23 displays the deck cross-section for the PFX-S20-LH15-W solution, while Figure 24 shows the constructive cross-section details.

### 4.4 Cost comparison

Comparing the different steel-concrete composite beams in different situations (span length and  $L/H$  ratios) enabled assessing the solution's performance indicator and determining which system is more economical for each case.

Without height restriction of the composite section, it was noted that the most economical solution for the 20 m spans is the pre-cambered composite beam with an  $L/H$  ratio of 15, as shown in Figure 25a. The chart takes into account the least economical solution with a maximum cost of 100%, with the percentage of the other cases being based on this value. For the 25-meter span, the pattern is repeated, with the pre-cambered beam solution presenting the most economical result in the overall context, as shown in Figure 25b.

**Table 3.** Geometric information of the sections obtained: composite beams with composite dowels.

Case	Section	Steel section				Connectors			Number of beams	Composite section					Steel weight/deck area (kg/m <sup>2</sup> )	Concrete volume/deck area (m <sup>3</sup> /m <sup>2</sup> )	
		h <sub>mr</sub> (mm)	b <sub>r</sub> (mm)	t <sub>r</sub> (mm)	t <sub>w</sub> (mm)	h <sub>d</sub> (mm)	e <sub>x</sub> (mm)	e <sub>y</sub> (mm)		H (mm)	b (mm)	h <sub>c</sub> (mm)	c <sub>o</sub> (mm)	c <sub>u</sub> (mm)			b <sub>c</sub> (mm)
PCB-S20-LH15-W	-	713.00	300.00	37.50	31.50	180.00	450.00	650.00	3	1333.00	4223.33	440.00	440.00	220.00	568.50	120.64	0.58
PCB-S20-LH20-L	W 920x420x656	403.50	431.00	62.00	34.50	180.00	450.00	912.00	4	1024.00	3167.50	440.00	440.00	270.00	827.50	190.78	0.64
PCB-S20-LH20-W	-	380.00	400.00	37.50	31.50	180.00	450.00	850.00	4	1000.00	3167.50	440.00	440.00	130.00	768.50	127.52	0.60
PCB-S20-LH25-W	-	180.00	720.00	44.50	37.50	180.00	450.00	1490.00	6	800.00	2111.67	440.00	440.00	135.50	1402.50	275.34	0.76
PCB-S25-LH15-W	-	1047.00	500.00	22.40	38.00	180.00	450.00	550.00	4	1667.00	3167.50	440.00	440.00	200.00	481.00	124.91	0.65
PCB-S25-LH20-W	-	425.00	400.00	44.50	31.50	180.00	450.00	850.00	4	1250.00	3167.50	440.00	440.00	200.00	768.50	147.29	0.70
PCB-S25-LH25-W	-	380.00	785.00	37.50	25.00	180.00	450.00	1620.00	7	1000.00	1810.00	440.00	440.00	335.50	1545.00	328.83	1.11
PCB-S30-LH15-W	-	1380.00	250.00	25.00	22.40	180.00	450.00	550.00	3	2000.00	4223.33	440.00	440.00	220.00	477.60	135.74	0.64
PCB-S30-LH20-W	-	880.00	405.00	44.50	22.40	180.00	450.00	860.00	4	1500.00	3167.50	440.00	440.00	835.50	787.60	181.66	0.82
PCB-S30-LH25-W	-	580.00	825.00	37.50	22.40	180.00	450.00	1700.00	7	1200.00	1810.00	440.00	440.00	542.50	1627.60	372.88	1.42

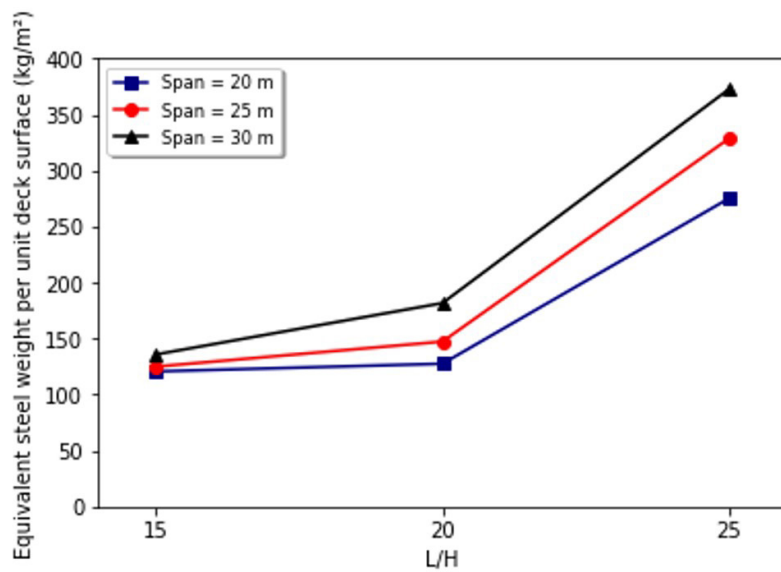


**Figure 19.** Equivalent steel weight per unit deck surface to slenderness ratio for beams with composite dowels.

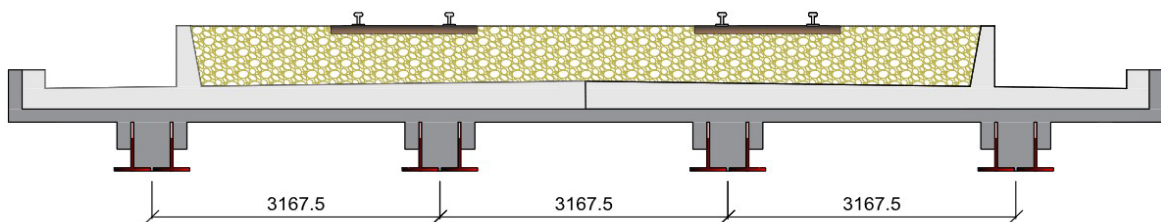


**Figure 20.** PCB-S20-LH20-W deck cross-section (dimensions in mm).

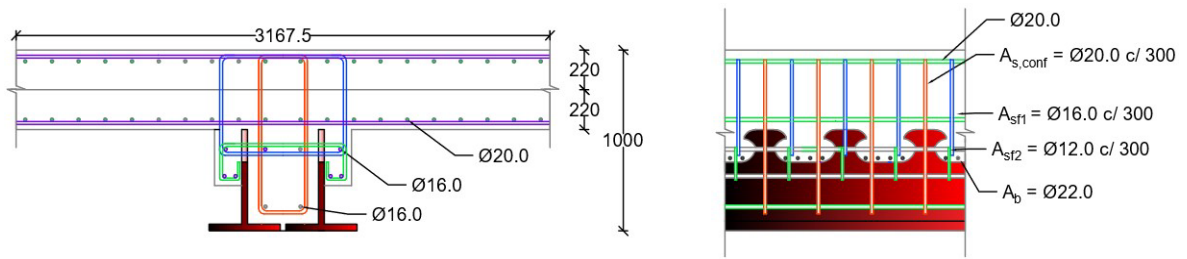


Figure 21. Construction details of PCB-S20-LH20-W solution (dimensions in mm).

Table 4. Geometric information of the sections obtained: pre-cambered composite beam.

Case	Steel section			Stud bolts			Bottom flange concrete					Composite section				
	h (mm)	bf,sup (mm)	tf,sup (mm)	bf,inf (mm)	tf,inf (mm)	t <sub>w</sub> (mm)	Studs/section	Type	Concrete volume/deck area (m <sup>3</sup> /m <sup>2</sup> )	Reinforcement weight/deck area (kg/m <sup>2</sup> )	Number of beams	H (mm)	b (mm)	h <sub>c</sub> (mm)	Steel weight/deck area (kg/m <sup>2</sup> )	Concrete volume/deck area (m <sup>3</sup> /m <sup>2</sup> )
PFX-S20-LH15-W	813.00	450.00	22.40	650.00	31.50	19.00	4	Ø22x150	0.04	2.98	4	1333.00	3167.50	440.00	111.21	0.44
PFX-S20-LH20-W	500.00	600.00	31.50	800.00	52.50	22.40	4	Ø22x150	0.03	4.97	5	1000.00	2534.00	440.00	217.01	0.44
PFX-S20-LH25-W	320.00	450.00	25.00	800.00	89.00	25.00	4	Ø22x150	0.04	6.71	9	800.00	1407.78	400.00	487.32	0.44
PFX-S25-LH15-W	1127.00	450.00	22.40	650.00	44.50	22.40	4	Ø22x150	0.04	2.24	3	1667.00	4223.33	440.00	116.36	0.44
PFX-S25-LH20-W	710.00	450.00	31.50	650.00	50.85	25.00	4	Ø22x150	0.08	4.47	6	1250.00	2111.67	440.00	233.34	0.44
PFX-S25-LH25-W	460.00	450.00	25.00	900.00	89.00	16.00	4	Ø22x150	0.13	9.94	10	1000.00	1267.00	440.00	598.86	0.44
PFX-S30-LH15-W	1430.00	450.00	22.40	637.00	44.50	22.40	4	Ø22x150	0.07	2.98	4	2000.00	3167.50	440.00	170.50	0.44
PFX-S30-LH20-W	960.00	450.00	31.50	650.00	44.50	25.00	4	Ø22x150	0.11	5.22	7	1500.00	1810.00	440.00	282.11	0.44
PFX-S30-LH25-W	630.00	450.00	25.00	1100.00	89.00	16.00	4	Ø22x150	0.23	12.43	10	1200.00	1267.00	440.00	725.70	0.44

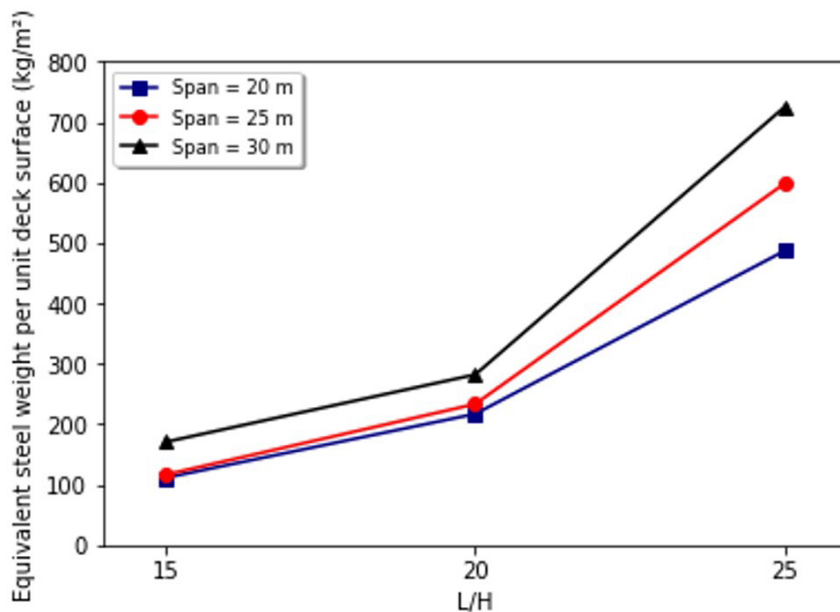


Figure 22. Equivalent steel weight per unit deck surface to slenderness ratio for pre-cambered composite beams.

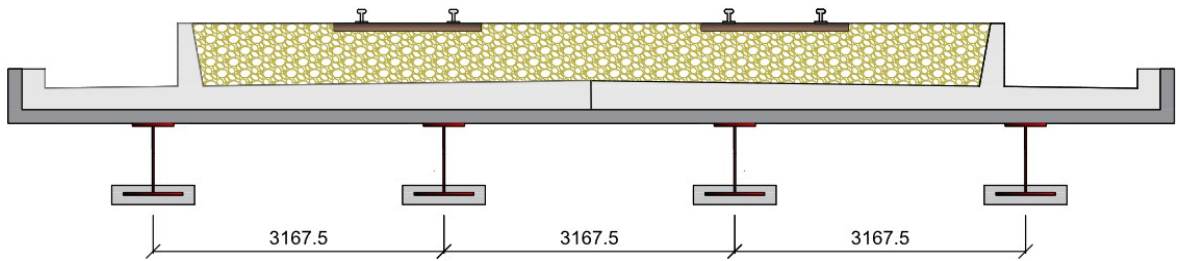


Figure 23. PFX-S20-LH15-W deck cross-section (dimensions in mm).

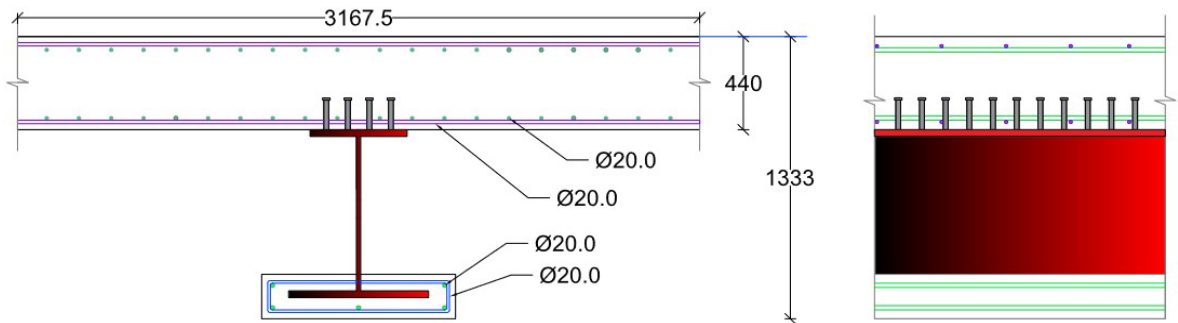
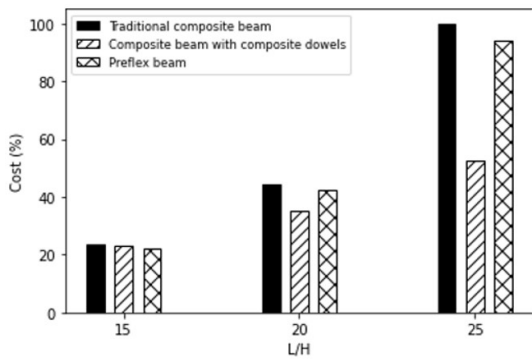
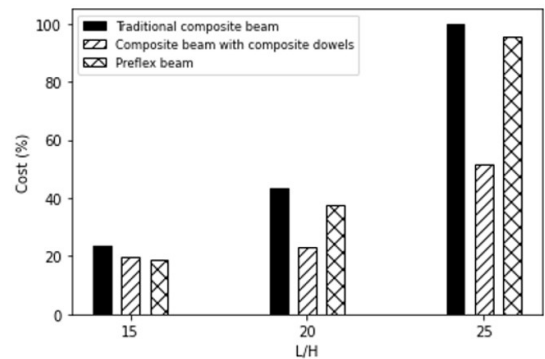


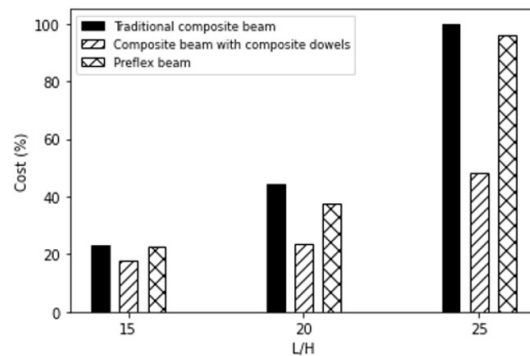
Figure 24. Construction details of PFX-S20-LH15-W solution (dimensions in mm).



(a)



(b)



(c)

Figure 25. Cost analysis: (a) 20-meter span; (b) 25-meter span; (c) 30-meter span.

For the first two spans analyzed, the composite beam with composite dowels presented a similar result as the Preflex beam for a deck slenderness ratio of 15. The cost difference in these cases was about 4%. However, for the 30 m, the composite beam with composite dowels presented the most economical result (Figure 25c).

For most bridge construction usually is necessary to limit the structure height, either for constructive or aesthetic reasons or even to guarantee the minimum vertical clearance under the bridge. Thus, the solutions were compared for their efficiency within the same deck slenderness ratio. The costs are higher when section height is reduced (Figure 25) since the structural stiffness is guaranteed by section mass increase, portraying more robust sections.

Considering the cases in which height restriction is necessary, Figure 26 displays the percentage costs of each composite beam solution in relation to the traditional system, separating them into different spans and  $L/H$  ratios. It is possible to notice that in all the cases evaluated, the unconventional solutions (composite beams with composite dowels and Preflex beams) presented lower costs than the traditional system.

In general, the composite beam with composite dowels was the most economical solution. For this system, the lower the cross-section height, the more economical the solution. The cost is up to half the traditional solution cost. This finding displays the composite beams with composite dowels as an interesting option from an economic point of view in situations where beam heights are limited.

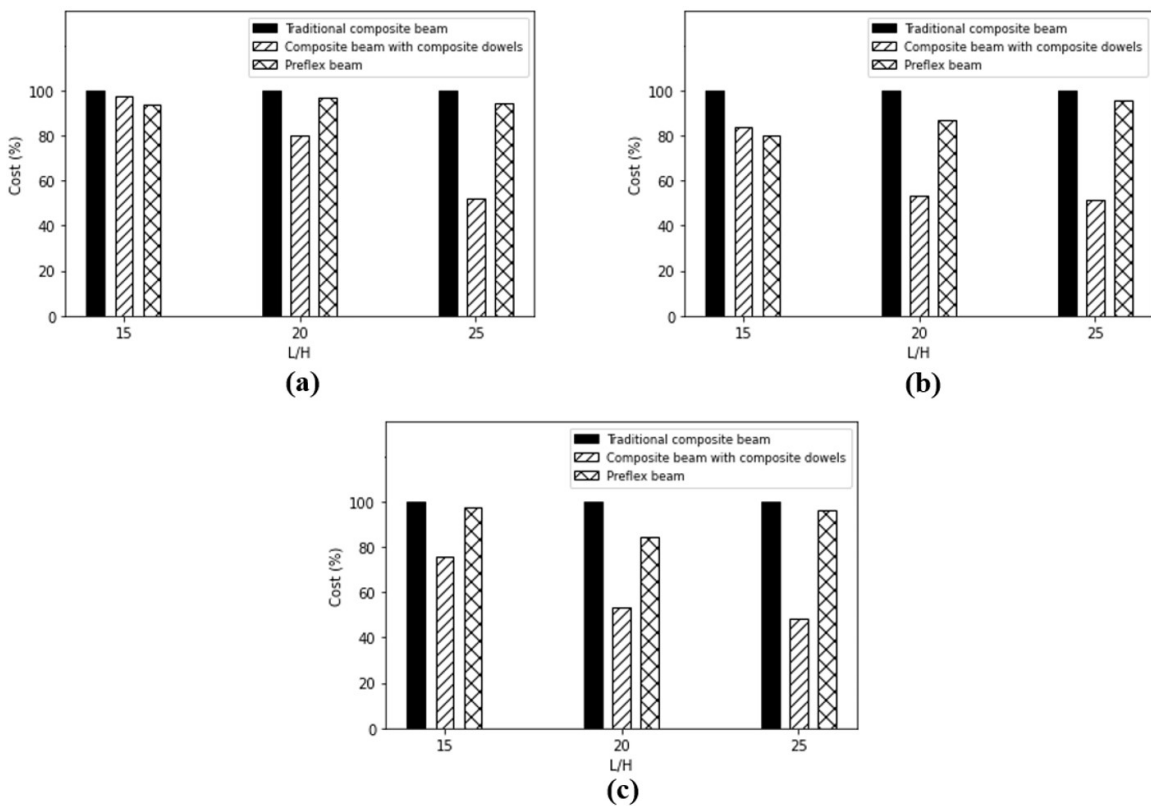


Figure 26. Cost analysis accounting for a beam height restriction: (a) 20-meter span, (b) 25-meter span; (c) 30-meter span.

In the pre-cambered composite beams case, the cost reduction compared to the traditional solution is slight for spans of 20 m. For this system, the most significant cost reductions were observed for the greater spans (25 m and 30 m) and  $L/H$  ratio of 20. It should be highlighted that for the 25-meter span and  $L/H$  of 15, the Preflex beam was even more economical than the composite beam with composite dowels.

The cost analysis displays the economic advantages of unconventional solutions for the analyzed cases. This fact corroborates the discussions in the literature, which point to composite beams with composite dowels and pre-cambered composite beams as viable alternatives for small and medium spans.

## 5 CONCLUSIONS

This paper presents a comparative study of different solutions for steel-concrete composite beams employed in bridge construction. The study aimed to obtain performance indicators of these technologies through various case studies, and the proposed case studies aimed to evaluate the applicability of unconventional composite beam systems. Thus, the paper content can be taken as a practical roadmap for future projects in the technical environment.

In order to design the composite beams, spreadsheets were developed based on the design proposed by the Eurocode provisions. However, to fill the design gaps in the current standards, the Z-26.4-56 [14] technical approval has covered the composite dowels design. Also, Morano and Mannini's method [7] has covered the procedures for calculating stresses and deflections due to creep and shrinkage effects for Preflex beams. Based on the analytical models, the design of the composite beam was proposed for the superstructure of a two-way simply-supported railway bridge.

For the composite beam with steel-plated connectors, a configuration with a double composite beam was chosen due to the railway deck dimensions and load conditions. This solution allows for a smaller number of beams and presents a significant constructive appeal since the steel profiles can be employed as concrete form, reducing the assembly time.

Sections with welded profiles were selected since they allow a more optimized cross-section and favor the comparison with other proposed solutions. For the same application, it was possible to verify a considerable reduction in the amount of steel, enabling savings when compared to laminated profiles. Furthermore, in countries with limited options for laminated profiles, such as Brazil, the adoption of welded plates is recommended. Nonetheless, verifying the fatigue strength of the welded connections between the steel web and flange is essential for this case.

In relation to structural performance, it was found that the decisive failure mode for design was related to the composite dowel fatigue. It was noticed the importance of ensuring adequate dimensions for the concrete cover,  $c_o$  and  $c_u$ , directly related to the occurrence of pry-out failure. In addition, it was observed that the longitudinal spacing between the connectors ( $e_x$ ) inadequate design can cause the concrete element failure by pry-out or shear.

The composite beams with continuous shear connectors presented better efficiency for deck slenderness ratios ( $L/H$ ) between 15 and 20, which can be considered a reasonable range for this technology pre-design. Compared to the traditional solution and the Preflex beams, this constructive system presents a suitable performance for an  $L/H$  ratio of 25.

The pre-cambered composite beams showed greater efficiency when applied to the case studies with greater beam height, with more satisfactory results when the  $L/H$  ratio is close to 15. Thus, this slenderness ratio can be considered a suitable pre-design range for the solution. In cases where there is no limitation on the height of the bridge section, Preflex beams demonstrate great competitiveness, being more economical for most spans. However, similar to the typical solution of a concrete slab and steel I-girders, this technology does not present satisfactory efficiency for high height restrictions, as displayed for a  $L/H$  ratio of 25.

From a cost analysis point of view, it was possible to identify that unconventional solutions have a lower material consumption, consequently implying cost reductions compared to the traditional system for the same span. The same happens when comparing solutions for the same deck slenderness ratio ( $L/H$ ). Thus, for bridges that require height restrictions, whether for constructive or aesthetic reasons, composite beams with composite dowels and Preflex beams result in more attractive options. This fact corroborates the discussions in the literature, which point to these two innovative solutions as viable alternatives for small and medium spans.

The composite beams with composite dowels provide a way to overcome the field complexities of installing stud bolts and characterizing an economical, rationalized, and time-saving process. The composite dowels also provide higher load-bearing capacity for static and cyclic load and ductility. On the other hand, the pre-cambered composite beam composition ensures gains in stiffness, flexural strength, and slenderness, being exceptionally attractive when deflection and vertical clearance are limited.

The composite beam alternatives presented in this paper display the same advantages as the traditional solution in terms of assembly and execution speed. The negative point is related to the structural elements' transport since, in these cases, the composite beams are fabricated in a controlled environment and then transported in their original form. Conversely, factory production leads to lower costs due to series production and automation, and reliability increments. Therefore, the application of these composite beams for bridge infrastructure is justified. This paper demonstrates the positive impact they could have as an innovative constructive method in countries such as Brazil.

As future developments, the authors suggest comparing the studied solutions for different span lengths and deck slenderness ratios. This inclusion, in addition to their verification of continuous bridges, would significantly broaden the knowledge regarding the application of these methods. Another interesting topic for future studies is a comparative study of innovative composite beam solutions described in this paper with precast reinforced concrete and prestressed concrete beams.



## ACKNOWLEDGEMENTS

The authors would like to acknowledge CNPq (grant # 132581/2018-3), CAPES, FAPEMIG (grant # APQ-01770-18 and APQ-02988-21, and FAPESP (grant # 2020/02350-2) for providing an essential part of the financial support needed to develop this paper. The opinions and conclusions presented in this paper are those of the authors and do not necessarily reflect the views of the sponsoring organizations.

## REFERENCES

- [1] D. Rademacher and N. Tilley, "Fast and easy dimensioning of robust and sustainable filler beam bridges," *Proc. Inst. Civ. Eng. Bridge Eng.*, vol. 173, no. 3, pp. 158–167, Sep 2020, <http://dx.doi.org/10.1680/jbren.19.00021>.
- [2] M. Kopp et al., "Composite dowels as shear connectors for composite beams – Background to the design concept for static loading," *J. Construct. Steel Res.*, vol. 147, pp. 488–503, Aug 2018, <http://dx.doi.org/10.1016/j.jcsr.2018.04.013>.
- [3] W. Lorenc, "The model for a general composite section resulting from the introduction of composite dowels," *Steel Constr.*, vol. 10, no. 2, pp. 154–167, May 2017, <http://dx.doi.org/10.1002/stco.201710019>.
- [4] M. Feldmann, M. Kopp, and D. Pak, "Composite dowels as shear connectors for composite beams – background to the german technical approval," *Steel Constr.*, vol. 9, no. 2, pp. 80–88, 2016, <http://dx.doi.org/10.1002/stco.201610020>.
- [5] W. Lorenc, R. Zanon, J. Berthelley, and G. Seidl, "An innovative solution for small span bridges - Precobeam," in *Innovative Steel Bridges Conference*, Innovative Steel Bridges Conference, Ed., 2014 [accessed Sept. 14, 2022]. [Online]. Available: <https://www.researchgate.net/publication/324038919>
- [6] D. Bae and K.-M. Lee, "Behavior of preflex beam in manufacturing process," *KSCE J. Civ. Eng.*, vol. 8, no. 1, pp. 111–115, Jan 2004, <http://dx.doi.org/10.1007/bf02829086>.
- [7] S. G. Morano and C. Mannini, "Preflex beams: a method of calculation of creep and shrinkage effects," *J. Bridge Eng.*, vol. 11, no. 1, pp. 48–58, 2006, <http://dx.doi.org/10.1061/ASCE1084-0702200611:148>.
- [8] G. Portela, U. Barajas, and J. A. Albarran-Garcia, *Analysis and Load Rating of Pre-Flex Composite Beams*. Vicksburg, USA: US Army Corps of Engineers, 2011.
- [9] S. Staquet, "Analyse et modelisation du comportement differe du beton. Application aux poutres mixtes, preflexchies et precontraintes," M.S. thesis, Universite Libre de Bruxelles, Brussels, 2004.
- [10] Christmann and Pfeifer. "The Preflex girder for bridge building." <https://www.cpbau.de/en/products/preflexgirder/> (accessed Sept. 01, 2022).
- [11] R. R. Santos, "Estudo comparativo de soluções para vigas mistas empregadas em obras de artes especiais," M.S. thesis, Universidade Federal de Minas Gerais, Belo Horizonte, Brasil, 2020.
- [12] R. R. Santos, H. Carvalho, R. F. Santos, R. B. Caldas, and T. Nogueira Bittencourt, "Composite dowels as shear connectors for steel-concrete composite beams on railway bridges," *Rev. Estrutura Aco*, vol. 12, no. 1, pp. 62–72, 2023.
- [13] European Committee for Standardization, *Design of Composite Steel and Concrete Structures. Part 2: General Rules and Rules for Bridges*, EN 1994-2, 2005.
- [14] Deutsches Institut für Bautechnik, *Allgemeine Bauartgenehmigung der Stahl-verbundträger mit Verbunddübelleisten in Klothoiden- und Puzzleform*, Z-26.4-56, 2018.
- [15] J. P. V. B. M. Fernandes, "Composite plate girder bridges. A state-of-the-art report of UK practice," M.S. thesis, Univerisity of Porto, Porto, Portugal, 2015. [Online]. Available: <http://www.fe.up.pt>
- [16] R. El Sarraf, D. C. Iles, A. Momtahan, D. Easey, and S. J. Hicks, *Steel-concrete composite bridge design guide*. Wellington, New Zealand: New Zealand Transport Agency, 2013.
- [17] B. T. Martin, "Highway bridges," in *Innovative Bridge Design Handbook: Construction, Rehabilitation and Maintenance*, A. Pipinato, Ed., Waltham: Elsevier, 2015, pp. 483–508.
- [18] D. C. Iles, *Design Guide for Steel Railway Bridges*. Berkshire, UK: Steel Construction Institute, 2004.
- [19] European Committee for Standardization, *Design of Composite Steel and Concrete Structures. Part 1-1: General Rules and Rules for Buildings*, EN 1994-1-1:2004, 2004.
- [20] European Committee for Standardization, *Basis of Structural Design*, EN 1990:2002., 2002.
- [21] European Committee for Standardization, *Design of Steel Structures. Part 1-1: General Rules and Rules for Buildings*, EN 1993-1-1, 2005.
- [22] European Committee for Standardization, *Design of Steel Structures. Part 1-5: Plated Structural Elements*, EN 1993-1-5, 2006.
- [23] European Committee for Standardization, *Design of Steel Structures. Part 1-9: Fatigue*, EN 1993-1-9, 2010.
- [24] European Committee for Standardization, *Design of Steel Structures. Part 2: Steel Bridges*, EN 1993-2, 2006.

- [25] European Committee for Standardization, *Design of Concrete Structures. Part 1-1: General Rules and Rules for Buildings*, EN 1992-1-1, 2004.
- [26] European Committee for Standardization, *Design of Concrete Structures. Part 2: Concrete Bridges - Design and Detailing Rules*, EN 1992-2: 2005, 2005.
- [27] F. Leonhardt, W. Andrä, H. Andrä, and W. Harre, "Neues, vorteilhaftes Verbundmittel für Stahlverbund-Tragwerke mit hoher Dauerfestigkeit," *Beton Stahlbetonbau*, vol. 82, no. 12, pp. 325–331, 1987.
- [28] H. S. Cardoso, O. P. Aguiar, R. B. Caldas, and R. H. Fakury, "Composite dowels as load introduction devices in concrete-filled steel tubular columns," *Eng. Struct.*, vol. 219, Sep 2020, <http://dx.doi.org/10.1016/j.engstruct.2020.110805>.
- [29] G. Seidl et al., *Prefabricated Enduring Composite Beams Based on Innovative Shear Transmission*. Brussels: European Commission, 2013. <https://www.doi.org/10.2777/9363>.
- [30] P. Kozioł, "Modern design of steel-concrete composite structures," *Budownictwo*, vol. 21, pp. 118–127, 2014.
- [31] U. B. Valdes, G. Portela, T. Stanton, W. Varela, and G. Velázquez, "Método de análisis para vigas preflexionadas basado en estándares de Norte América," *Rev Int Desastres Naturales, Accidentes Infraestruct. Civ.*, vol. 10, no. 2, pp. 95–105, 2010.
- [32] C. Mannini, "Valutazione degli effetti di fluage e ritiro e problemi di ottimizzazione delle sezioni per impalcati ferroviari," M.S. thesis, Università Degli Studi di Firenze, Florence, 2001.
- [33] European Committee for Standardization, *Actions on structures. Part 2: Traffic loads on bridges*, EN 1991-2:2003, 1991.
- [34] A. K. Binjola, "Load distribution in girders bridges by different methods," M.S. thesis, University of Roorkee, Roorkee, 1988.

---

**Author contributions:** RRS: data curation, formal analysis, investigation, methodology, writing; HC: conceptualization, formal analysis, methodology, resources, supervision, revision; RFS: formal analysis, investigation, writing; TNB and RBC: validation, visualization, revision.

**Editors:** Rebecca Gravina, Guilherme Aris Parsekian.

**APPENDIX A.1: ULS, SLS, AND FLS RESULTS: TRADITIONAL SOLUTION.**

Case	Short-term						Long-term							
	ULS		SLS		FLS		ULS		SLS		FLS			
	MplRd/Me d or $\sigma_d/\sigma_{Ed}$	V <sub>Rd</sub> / V <sub>L,Rd</sub>	V <sub>L,Rd</sub> / V <sub>L,Rd</sub>	Displacement (mm)	V <sub>L,Rd</sub> / V <sub>L,Rd</sub>	$\Delta\tau_c/\lambda\phi\Delta\tau_c$	$\Delta\sigma_{cf}/\lambda\phi\Delta\sigma_{cf}$	MplRd/Me <sub>d</sub> ou $\sigma_d/\sigma_{Ed}$	V <sub>Rd</sub> / V <sub>L,Rd</sub>	V <sub>L,Rd</sub> / V <sub>L,Rd</sub>	Displacement (mm)	V <sub>L,Rd</sub> / V <sub>L,Rd</sub>	$\Delta\tau_c/\lambda\phi\Delta\tau_c$	$\Delta\sigma_{cf}/\lambda\phi\Delta\sigma_{cf}$
TRA-V20-LH15-S	1.63	1.52	1.40	25.46	1.48	1.49	2.93	1.50	1.38	1.30	32.50	1.47	1.47	2.69
TRA-V20-LH20-S	1.53	1.09	1.10	27.07	1.17	1.15	4.60	1.50	1.09	1.03	38.92	1.17	1.15	4.30
TRA-V20-LH25-S	1.24	1.95	1.18	27.57	1.25	1.24	8.76	1.12	1.73	1.12	47.27	1.27	1.26	8.78
TRA-V25-LH15-S	1.65	1.13	1.39	31.42	1.48	1.63	3.11	1.47	1.12	1.35	39.76	1.53	1.69	2.92
TRA-V25-LH20-S	1.54	1.44	1.31	32.16	1.39	1.48	4.92	1.46	1.35	1.27	46.28	1.44	1.54	4.71
TRA-V25-LH25-S	1.24	1.53	1.03	32.02	1.09	1.19	9.50	1.12	1.44	1.03	54.43	1.16	1.28	9.57
TRA-V30-LH15-S	1.61	1.30	1.01	38.39	1.07	1.27	3.18	1.41	1.22	1.01	48.87	1.15	1.36	3.00
TRA-V30-LH20-S	1.48	1.66	1.33	38.46	1.41	1.63	5.14	1.41	1.55	1.37	55.15	1.55	1.78	4.91
TRA-V30-LH25-S	1.19	1.61	1.42	36.05	1.50	1.79	10.95	1.06	1.51	1.45	62.51	1.63	1.95	11.13

**APPENDIX A.2. ULS, SLS, AND FLS RESULTS: COMPOSITE BEAMS WITH COMPOSITE DOWELS.**

Case	Short-term								Long-term						
	ULS			SLS			FLS		ULS			SLS			FLS
	M <sub>pl,Rd</sub> /M <sub>ed</sub> or σ <sub>a</sub> /σ <sub>Ed</sub>	V <sub>Rd</sub> /V <sub>L,Rd</sub>	V <sub>L,Rd</sub> /V <sub>L,Rd</sub>	Displacement (mm)	V <sub>L,Rd</sub> /V <sub>L,Rd</sub>	Δτ <sub>c</sub> /λφΔτ	Δσ <sub>c,lf</sub> /λφΔσ <sub>E,lf</sub>	M <sub>pl,Rd</sub> /M <sub>ed</sub> or σ <sub>a</sub> /σ <sub>Ed</sub>	V <sub>Rd</sub> /V <sub>L,Rd</sub>	V <sub>L,Rd</sub> /V <sub>L,Rd</sub>	Displacement (mm)	V <sub>L,Rd</sub> /V <sub>L,Rd</sub>	Δτ <sub>c</sub> /λφΔτ	Δσ <sub>c,lf</sub> /λφΔσ <sub>E,lf</sub>	
PCB-V20-LH15-S	2.17	4.93	1.02	16.61	1.26	1.55	5.50	2.17	5.00	3.79	23.51	4.68	1.14	4.25	
PCB-V20-LH20-L	1.42	3.53	1.01	20.65	1.25	1.49	7.14	1.42	3.56	1.57	30.95	1.93	1.06	5.17	
PCB-V20-LH20-S	1.63	3.29	1.00	26.54	1.24	1.53	5.06	1.63	3.32	2.10	39.73	2.59	1.05	3.56	
PCB-V20-LH25-S	1.10	2.17	1.25	27.43	1.54	1.88	8.54	1.48	2.17	1.49	45.36	1.84	1.19	5.47	
PCB-V25-LH15-S	1.94	4.70	1.56	21.45	1.92	1.70	5.19	1.94	4.74	2.74	28.21	3.39	1.09	3.67	
PCB-V25-LH20-S	1.60	2.84	1.10	31.31	1.36	1.80	5.67	1.60	2.87	3.38	31.79	4.16	1.21	3.89	
PCB-V25-LH25-S	1.00	3.07	1.50	31.43	1.84	1.86	9.53	1.84	3.07	8.45	34.79	10.37	1.05	5.41	
PCB-V30-LH15-S	1.59	4.63	1.16	29.69	1.43	1.57	4.69	1.59	4.71	2.67	38.62	3.29	1.07	3.60	
PCB-V30-LH20-S	1.46	3.56	1.50	35.39	1.85	1.66	6.35	1.46	3.59	1.44	42.96	1.77	1.06	4.40	
PCB-V30-LH25-S	1.45	3.34	1.55	36.14	1.89	1.99	10.08	1.09	3.34	1.24	39.70	1.52	1.18	6.20	

**APPENDIX A.3. ULS, SLS, AND FLS RESULTS: PRE-CAMBERED COMPOSITE BEAMS.**

Case	ULS				SLS			FLS		
	$M_{pl,Rd}/M_{ed}$ or $\sigma_s/\sigma_{Ed}$	$V_{Rd}/V_{L,Rd}$	$V_{L,Rd}/V_{L,Rd}$ Deck	$V_{L,Rd}/V_{L,Rd}$ C1	Displacement (mm)	$V_{L,Rd}/V_{L,Rd}$ Deck	$V_{L,Rd}/V_{L,Rd}$ C1	$\Delta\tau_c/\lambda\varphi\Delta\tau_c$ Deck	$\Delta\tau_c/\lambda\varphi\Delta\tau_c$ C1	$\Delta\sigma_{c,lf}/\lambda\varphi\Delta\sigma_{c,lf}$
PFX-V20-LH15-S	1.31	1.31	1.33	1.05	17.83	1.41	1.11	1.43	1.13	5.09
PFX-V20-LH20-S	2.35	1.05	1.18	1.07	27.22	1.26	1.14	1.26	1.14	5.33
PFX-V20-LH25-S	2.72	1.06	1.11	1.93	29.67	1.18	2.04	1.18	2.04	9.81
PFX-V25-LH15-S	1.39	1.62	1.27	1.07	31.27	1.34	1.13	1.19	1.00	3.91
PFX-V25-LH20-S	1.31	1.66	1.03	1.13	31.67	1.09	1.20	1.20	1.32	6.08
PFX-V25-LH25-S	2.40	1.01	1.19	1.10	35.21	1.26	1.16	1.43	1.32	12.69
PFX-V30-LH15-S	1.35	1.26	1.35	1.25	24.55	1.44	1.32	1.74	1.60	6.22
PFX-V30-LH20-S	1.28	2.24	1.24	1.17	35.34	1.31	1.24	1.55	1.47	6.55
PFX-V30-LH25-S	2.19	1.14	1.20	1.17	38.76	1.26	1.24	1.61	1.58	16.00